

Metastatic Pulmonary Hepatoid Carcinoma with Vascular Complications and Transplanted Kidney

.....

By Matthias Stefan May, MD
Department of Radiology, University Hospital Erlangen, Germany

History

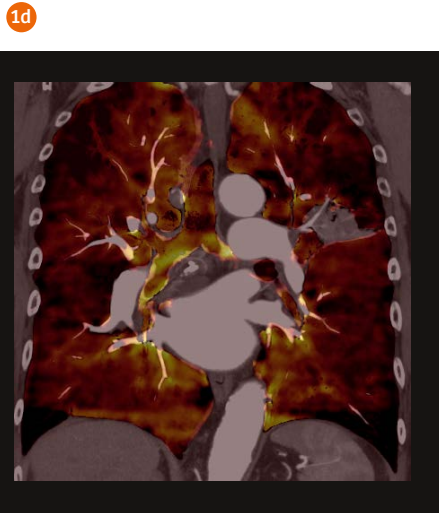
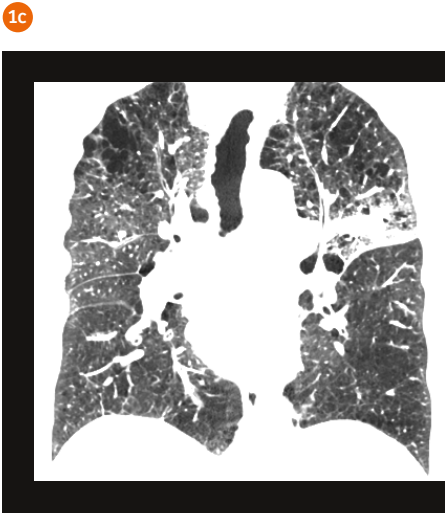
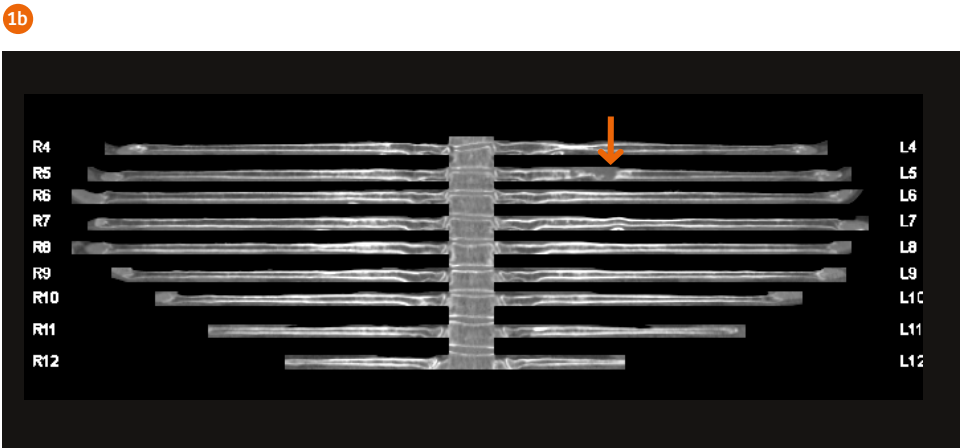
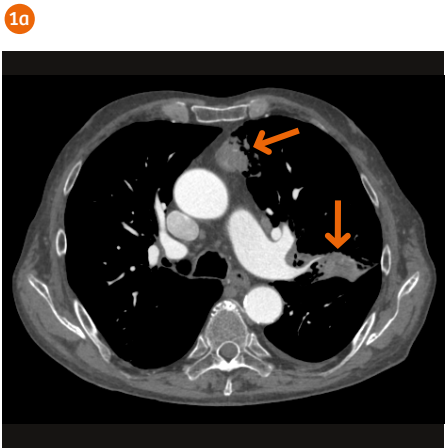
A 74-year-old male patient came to the hospital complaining of increasing shortness of breath. A chest radiograph showed a triangular opacity in the periphery of the left lung, possibly indicating a pulmonary embolism (PE). An abdominal ultrasound exam-

ination revealed a possible abdominal aortic aneurysm (AAA). The patient had a history of right hip replacement and chronic claudication with right lower limb pain. A decade ago, he underwent kidney transplantation, and currently had an estimated glomerular

filtration rate (GFR) of 70.3 mL/min/1.73m². TwinBeam Dual Energy (TBDE) CT was performed to rule out PE and to investigate the systemic arterial circulation, using only a single bolus injection and thereby keeping the iodine charge as low as possible.

Examination Protocol

Scanner	SOMATOM go.Top		
Scan area	Whole body	Rotation time	0.33 s
Scan mode	TBDE	Pitch	0.3
Scan length	1563.8 mm	Slice collimation	64 × 0.6 mm
Scan direction	Cranio-caudal	Slice width	0.8 mm
Scan time	44.7 s	Reconstruction increment	0.6 mm
Tube voltage	Au/Sn120 kV	Reconstruction kernel	Qr40, Bv36 and Br56 (each with ADMIRE 3)
Effective mAs	238 mAs	Contrast	350 mg/mL
Dose modulation	CARE Dose4D™	Volume	100 mL + 30 mL saline
CTDI _{vol}	6.6 mGy	Flow rate	5 mL/s
DLP	1064 mGy cm	Start delay	Aortic bolus tracking with 100 HU + 10s



1 Axial (Fig. 1a) and coronal (Fig. 1c) views show two consolidations in the upper left lobe in segments 2 and 3 (arrows), thickening of the surrounding septa, obstruction of the segmental bronchus 2, and enlarged lymphatic nodes in the left hilum. Lung PBV image (Fig. 1d) shows areas with defects in PBV corresponding to emphysema and distal to the obstruction of the bronchus. A rib unfolding image (Fig. 1b) easily reveals a solitary lytic bone metastasis in the left fifth rib (arrow, ribs #1–3 were incompletely covered in the scan range).

Diagnosis

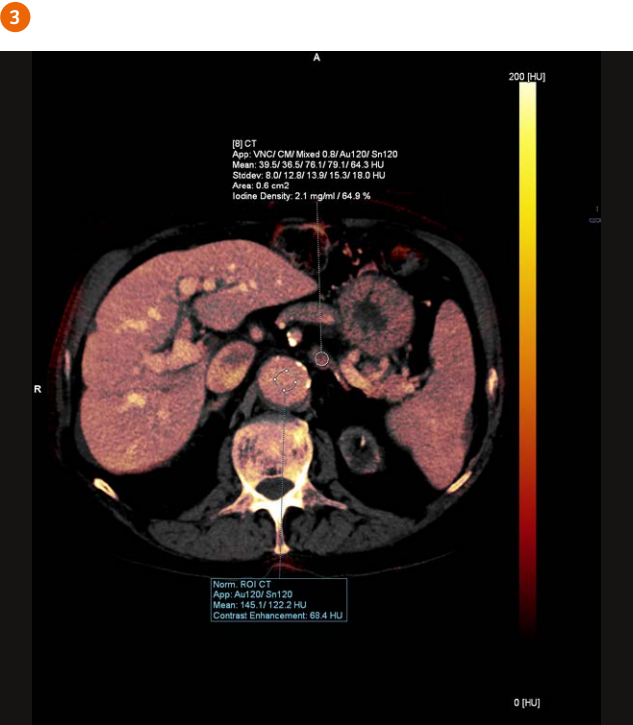
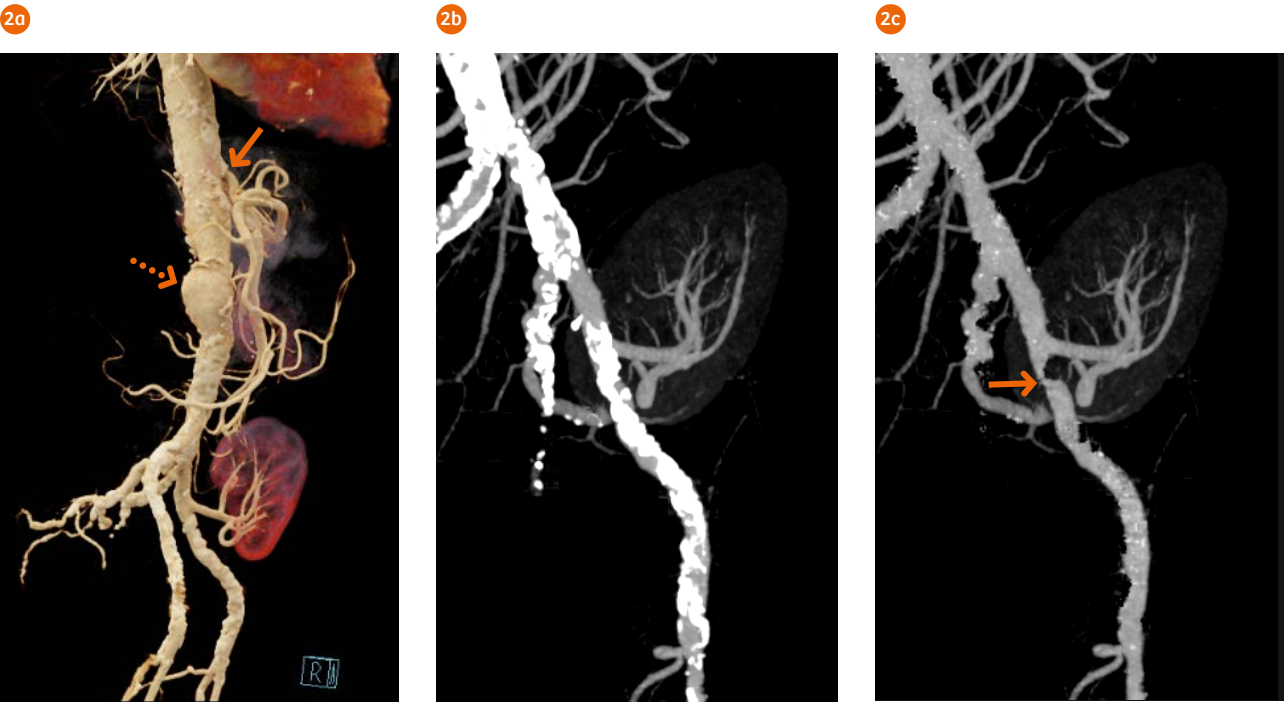
CT images revealed two consolidations in the upper left lobe in segments 2 and 3, with thickening of the surrounding septa, obstruction of the segmental bronchus 2, and enlargement of the lymphatic nodes in the left hilum. These findings suggested a bronchial carcinoma with perifocal lymphangitic carcinomatosis and ipsilateral lymphatic metastases. No signs of PE were present. Histopathological workup via endobronchial biopsy resulted in a final diagnosis of pulmonary hepatoid carcinoma (G3). A solitary lytic bone metastasis in the left fifth rib was visualized. The left adrenal gland was enlarged, hyperdense and contrast enhanced, suggesting a metastasis. The infrarenal abdominal aorta was enlarged and

partially thrombotic, measuring 4.8 × 4.5 cm in size, confirming an AAA. A moderate stenosis of the proximal celiac artery and a severe stenosis of the left external iliac artery, right below the well-perfused transplanted kidney in the left iliac fossa, were seen. The right superficial femoral artery was occluded in the adductor canal over a length of 5 cm, causing a delay in the blood flow of the popliteal artery via collaterals. A right prosthetic component was correctly positioned with no signs of fracture or dislocation.

Comments

Hepatoid carcinoma is a rare extrahepatic tumor with histomorphological features similar to hepatocellular carcinoma. Pulmonary hepatoid carcinoma

is extremely rare and, once detected, requires differential diagnosis from metastatic hepatocellular carcinoma. In this case, one of the challenges for the radiologist was to complete a workup of several clinical tasks with a single injection of contrast agent: rule out a PE, evaluate lung perfusion, assess staging of bronchial carcinoma, differentiate lesion characters in the adrenal gland, evaluate an AAA as well as the left iliac kidney transplant, and determine grading of peripheral arterial disease with visualization for clinical presentation. TBDE allows the simultaneous acquisition of high and low energy spectra in a single scan. The dataset can then be processed using various DE applications. DSA-like CT angiographic images can be easily reformatted, using syngo.CT DE Direct Angio, to remove



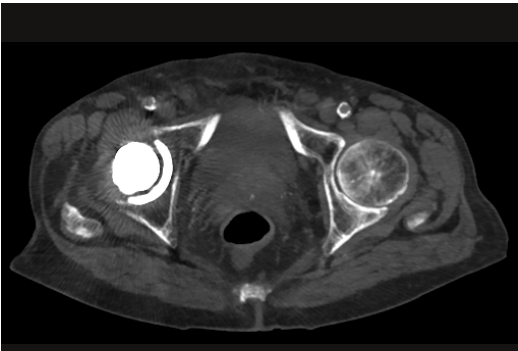
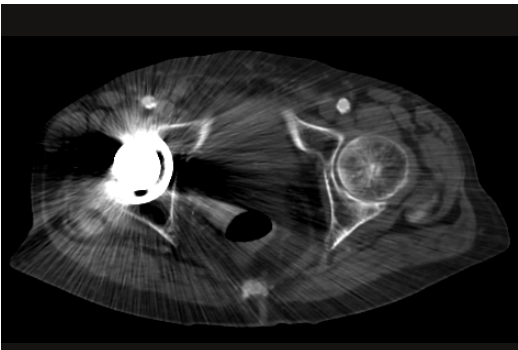
2 A cinematic VRT image (Fig. 2a) shows an AAA (dotted arrow), a moderate stenosis of the proximal celiac artery (arrow), and the well-perfused transplanted kidney. MIP images (Fig. 2b and Fig. 2c) show that a severe stenosis of the left external iliac artery, right below the renal artery of the transplanted kidney that cannot be visualized in standard reconstructions due to severe calcifications (Fig. 2b), is clearly depicted after calcium removal (Fig. 2c, arrow).

3 An axial iodine map show an enlarged and enhanced left adrenal gland, measuring 39.5 HU in density in VNC and 76.1 HU in portal venous phase, with an iodine uptake of 2.1 mg/mL, suggesting a metastasis.

the bony structures. Virtual noncontrast (VNC) images and iodine maps can be created using *syngo*.CT DE Virtual Unenhanced to present and quantify the iodine uptake. The image contrast can be significantly enhanced using *syngo*.CT DE Monoenergetic Plus

(Mono+) at lower keV settings. The perfused blood volume (PBV) of the lungs can also be evaluated using *syngo*.CT DE Lung PBV. Additionally, the *syngo* CT Vascular application allows the generation of a curved MPR along the centerline of the abdominal

aorta for an accurate measurement of its size, and removal of the calcified plaques for clear visualization of the true vessel lumen and the severity of the stenosis. The metal artifacts caused by the hip prosthesis, which impact the view of the surrounding



4 A MIP image acquired at 120 kV after bone removal (Fig. 4a) shows extensive calcified plaques in the whole body CTA. Image contrast is significantly enhanced using Mono+ at 45 keV, and the vessel lumen is clearly depicted after calcium removal (Fig. 4b). The right superficial femoral artery is occluded over a length of 5 cm (Fig. 4b, arrow), causing a delay of the blood flow in the popliteal artery via collaterals. Both images are displayed with the same window levels.

5 Axial images show that severe metal artifacts (Fig. 5a), affecting the visualization of the hip, pelvis and the iliac arteries, are significantly removed by iMAR application (Fig. 5b).

anatomical structures, can be significantly reduced by iterative Metal Artifact Reduction (iMAR). All these applications help the physicians make a confident diagnosis and plan further treatment. ●

The outcomes by Siemens Healthineers customers described herein are based on results that were achieved in the customer's unique setting. Since there is no "typical" hospital and many variables exist (e.g., hospital size, case mix, level of IT adoption), there can be no guarantee that other customers will achieve the same results.